

# Bis-Tridentate Ir(III) Metal Phosphors for Efficient Deep-Blue Organic Light-Emitting Diodes

Hsin-Hung Kuo, Yi-Ting Chen, Leon R. Devereux, Chung-Chih Wu,\* Mark A. Fox,\*  
Chu-Yun Kuei, Yun Chi,\* and Gene-Hsiang Lee

**Emissive Ir(III) metal complexes possessing two tridentate chelates (bis-tridentate) are known to be more robust compared to those with three bidentate chelates (tris-bidentate). Here, the deep-blue-emitting, bis-tridentate Ir(III) metal phosphors bearing both the dicarbene pincer ancillary such as 2,6-diimidazolylidene benzene and the 6-pyrazolyl-2-phenoxy pyridine chromophoric chelate are synthesized. A deep-blue organic light-emitting diode from one phosphor exhibits Commission Internationale de l'Eclairage (CIE<sub>(x,y)</sub>) coordinates of (0.15, 0.17) with maximum external quantum efficiency (max. EQE) of 20.7% and EQE = 14.6% at the practical brightness of 100 cd m<sup>-2</sup>.**

The third-row transition-metal complexes are pivotal to the development of organic light-emitting diodes (OLEDs), which can be fabricated with unitary internal quantum efficiencies, attributed to the heavy-atom-induced spin-orbital coupling that allow fast singlet-triplet intersystem crossing and efficient phosphorescence at room temperature (RT).<sup>[1]</sup> However, the main barrier is the lack of stable and efficient blue-emitting phosphors, for

which the developments still lag behind the green and red counterparts due to the intrinsically wider energy gaps.<sup>[2]</sup> Efficient blue-emitters are expected to reduce power consumption and improve color gamut; therefore, they have emerged as one paradigm of the full-color OLED displays and solid-state lighting.<sup>[3]</sup>

Among the various known blue phosphors, the sky-blue emitter Irpic is considered to be the archetypal design; hence, its modulation is at the forefront of modern research in OLEDs.<sup>[4]</sup> OLEDs made with Irpic typically have Commis-

sion Internationale de l'Eclairage (CIE<sub>(x,y)</sub>) coordinates of (0.17, 0.34) which is far from the National Television Standards Committee pure blue values of (0.14, 0.08). Progress with blue phosphors is further complicated by other issues, such as chemical and physical stabilities, emission quantum yield, and relative radiative lifetime. Moreover, almost all reports of decent blue phosphors were focused on the so-called tris-bidentate architectures, i.e., with either three bidentate cyclometalates of higher ligand-centered  $\pi\pi^*$  energy gap or two of these cyclometalate plus a third bidentate ancillary.<sup>[5]</sup> However, these complexes suffer from possible chelate dissociation upon excitation, giving inferior device performances and longevity.<sup>[6]</sup>

Recently, Whittle and Williams,<sup>[7]</sup> Haga and co-workers,<sup>[8]</sup> De Cola and co-workers,<sup>[9]</sup> and Esteruelas and co-workers<sup>[10]</sup> have independently conducted studies on emitters bearing two tridentate chelates; namely bis-tridentate metal complexes. This class of molecular designs is expected to be more robust and should be of higher efficiency attributed to the concomitant higher rigidity versus the traditional design bearing three bidentate chelates.<sup>[11]</sup> Despite the obvious advantages, these associated studies were greatly hampered by the lack of systematic syntheses and poor performances on OLEDs. These difficulties were recently solved by proper selection of chelates to give the charge-neutral architecture<sup>[12]</sup> and the installment of a higher field strength coordination unit.<sup>[13]</sup>

One known bis-tridentate metal complex is the sky-blue Ir(III) phosphor [Ir(mimf)(pzpyph<sup>F</sup>)] (SB = "sky-blue"),<sup>[14]</sup> where the tridentate 6-pyrazolyl-2-phenylpyridine (pzpyph<sup>F</sup>) and pincer dicarbene chelate (mimf) act as the chromophoric and ancillary chelates, respectively (**Scheme 1**). These ligands control the emission color and give the greater ligand field strength needed for the efficient phosphors.<sup>[15]</sup> Hence, the OLED derived from SB gave maximum external quantum efficiency (max. EQE) of 27% and EQE of 24% at the practical

H.-H. Kuo, C.-Y. Kuei, Prof. Y. Chi  
Department of Chemistry  
National Tsing Hua University  
Hsinchu 30013, Taiwan  
E-mail: ychi@mx.nthu.edu.tw

Y.-T. Chen, Prof. C.-C. Wu  
Graduate Institute of Electronics Engineering  
and Department of Electrical Engineering  
National Taiwan University  
Taipei 10617, Taiwan  
E-mail: wucc@ntu.edu.tw

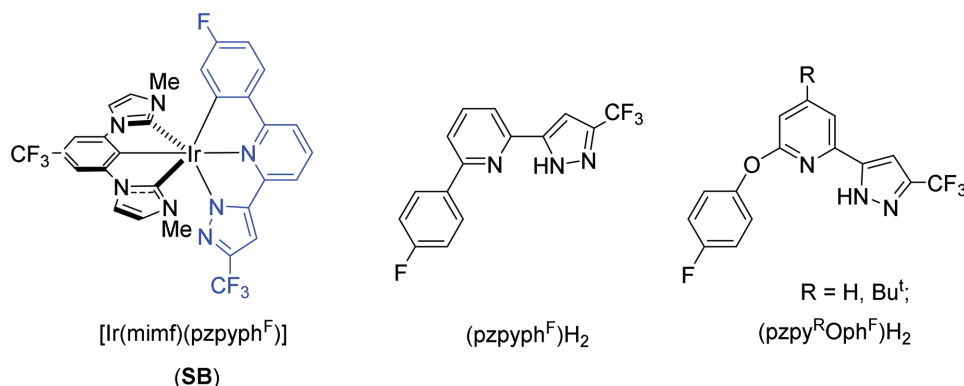
L. R. Devereux, Dr. M. A. Fox  
Department of Chemistry  
Durham University  
South Road, Durham DH1 3LE, UK  
E-mail: m.a.fox@durham.ac.uk

Prof. G.-H. Lee  
Instrumentation Center  
National Taiwan University  
Taipei 10617, Taiwan

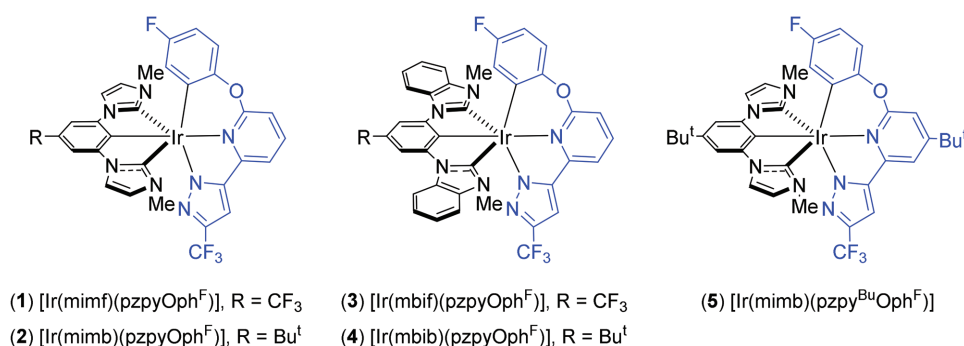
© 2017 The Authors. Published by WILEY-VCH Verlag GmbH & Co. KGaA, Weinheim. This is an open access article under the terms of the Creative Commons Attribution-NonCommercial License, which permits use, distribution and reproduction in any medium, provided the original work is properly cited and is not used for commercial purposes.

 The ORCID identification number(s) for the author(s) of this article can be found under <https://doi.org/10.1002/adma.201702464>.

DOI: 10.1002/adma.201702464



**Scheme 1.** Structural drawings of bis-tridentate Ir(III) complex SB and corresponding dianionic chromophoric chelates.



**Scheme 2.** Molecular structures of the studied bis-tridentate Ir(III) metal complexes 1–5.

brightness of  $100 \text{ cd m}^{-2}$ . However, this device has  $\text{CIE}_{(x,y)}$  coordinates of (0.18, 0.40) which is less satisfactory than OLEDs fabricated from FIrpic.

Both pyridyl and fluorophenyl units in the chromophoric chelate in this bis-tridentate Ir(III) phosphor SB had shown significant contributions to the frontier orbitals.<sup>[14]</sup> Thus, we decided to break the  $\pi$ -conjugation between the pyridyl and fluorophenyl units with the intention of widening the highest occupied molecular orbital (HOMO)–lowest unoccupied molecular orbital (LUMO) energy gap (HLG) in our bis-tridentate Ir(III) template for a bluer emission.<sup>[16]</sup> The  $\text{pzpyph}^{\text{F}}$  chromophoric chelate<sup>[14]</sup> was deliberately replaced with the phenoxy-containing chelate (cf.  $\text{pzpy}^{\text{R}}\text{Oph}^{\text{F}}\text{H}_2$ ,  $\text{R} = \text{H}, \text{Bu}^{\text{t}}$ ) which proved to be simple to synthesize and can indeed be manipulated with various substituents if desired (Scheme 1). Indeed, these new bis-tridentate Ir(III) phosphors have given deep-blue emissions. As a proof-of-concept, they were applied in the fabrication of deep-blue-emitting OLEDs, featuring comparable or an even better performance versus the deep-blue-emitting OLEDs based on traditional tris-bidentate Ir(III) metal phosphors.<sup>[17]</sup>

The pincer dicarbene ancillary chelate (e.g., 2,6-diimidazolylidene or 2,6-dibenzimidazolylidene benzene) is retained in the molecules for the higher metal-chelate bond strength. Syntheses of blue-emitting Ir(III) metal complexes 1–5 required both tridentate prochelates, i.e., monoanionic bis(imidazolylidene) benzene and dianionic 6-pyrazolyl-2-phenoxy pyridine (Scheme 2). The pincer dicarbene chelate

precursors are  $\text{PF}_6^-$  salts of  $(\text{mimf})\text{H}_3^{2+}$ ,  $(\text{mimb})\text{H}_3^{2+}$ ,  $(\text{mbif})\text{H}_3^{2+}$ , and  $(\text{mbib})\text{H}_3^{2+}$  (Scheme S1, Supporting Information) which were synthesized using literature procedures.<sup>[18]</sup> The dianionic chromophoric chelate precursors  $(\text{pzpy}^{\text{R}}\text{Oph}^{\text{F}})\text{H}_2$ ,  $\text{R} = \text{H}$  and  $\text{Bu}^{\text{t}}$ , were prepared from Cu-catalyzed arylation of phenols<sup>[19]</sup> followed by Claisen condensation and hydrazine cyclization (Scheme S2, Supporting Information).

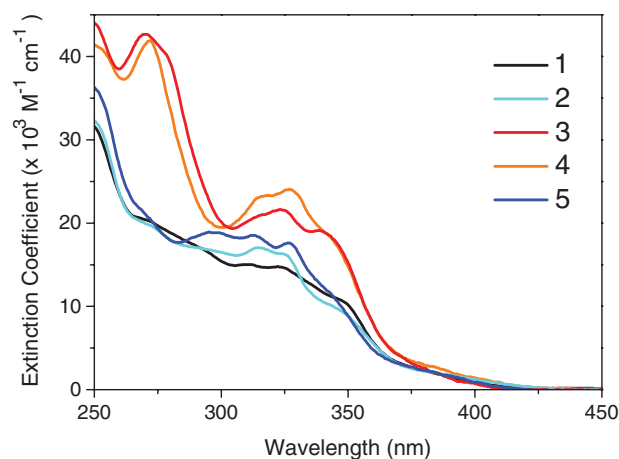


**Figure 1.** Absorption spectra of Ir(III) complexes 1–5 recorded in  $\text{CH}_2\text{Cl}_2$  at RT.

**Table 1.** Photophysical and electrochemical data of the studied Ir(III) phosphors 1–5.

	abs $\lambda_{\text{max}}$ ( $\epsilon$ ) <sup>a)</sup> [nm] ( $\times 10^{-3} \text{ M}^{-1} \text{ cm}^{-1}$ )	PL $\lambda_{\text{max}}$ <sup>a)</sup> [nm]	FWHM <sup>b)</sup> [cm <sup>-1</sup> ]	$\Phi$ <sup>a)</sup> [%]	$\tau_{\text{obs}}$ <sup>a)</sup> [ $\mu\text{s}$ ]	$E^{\text{ox}}_{1/2}$ ( $\Delta E_p$ ) <sup>c)</sup> [V]	$E^{\text{re}}_{\text{pc}}$ <sup>d)</sup> [V]
1	323 (14.7), 348 (10.6), 384 (2.0), 418 (0.2)	447 (sh), 471, 505 (sh)	3700	81	25.1	0.67 (0.08)	−2.92
2	326 (16.1), 349 (9.1), 388 (1.9), 420 (0.4)	444 (sh), 478, 505 (sh)	3500	82/81 <sup>e)</sup>	4.42/3.83 <sup>e)</sup>	0.53 (0.07)	−2.94
3	323 (21.6), 345 (17.8), 387 (1.8), 404 (0.4)	447 (sh), 473, 506 (sh)	3330	68	61.2	0.80 (0.08)	−2.80
4	326 (24.0), 345 (17.5), 387 (2.4), 419 (0.4)	448 (sh), 473, 506 (sh)	3670	79	18.6	0.62 (0.07)	−2.94
5	327 (17.5), 346 (10.2), 386 (1.8), 412 (0.3)	448 (sh), 472, 505 (sh)	3500	72/91 <sup>e)</sup>	8.66/3.98 <sup>e)</sup>	0.52 (0.08)	−3.10

<sup>a)</sup>UV–vis spectra, photoluminescence (PL) spectra, lifetime and quantum yields were recorded in  $\text{CH}_2\text{Cl}_2$  at a concentration of  $10^{-5} \text{ M}$ ; <sup>b)</sup>FWHM: full width at half maxima of PL emission in  $\text{cm}^{-1}$ ; <sup>c)</sup> $E^{\text{ox}}_{1/2}$  refers to  $[(E_{\text{pa}} + E_{\text{pc}})/2]$ , where  $E_{\text{pa}}$  and  $E_{\text{pc}}$  are the anodic and cathodic wave, respectively, for the oxidation half-wave potential and referenced to the ferrocene redox couple ( $\text{FcH}/\text{FcH}^+ = 0 \text{ V}$ ),  $\Delta E_p = E_{\text{pa}} - E_{\text{pc}}$  conducted in  $\text{CH}_2\text{Cl}_2$  solution; <sup>d)</sup> $E^{\text{re}}$  is the cathodic wave potential for the irreversible reduction wave referenced to the ferrocene redox couple ( $\text{FcH}/\text{FcH}^+ = 0 \text{ V}$ ) in tetrahydrofuran (THF) solution; <sup>e)</sup>Photoluminescence quantum yields (PLQYs) and excited-state lifetimes when doped in thin films of the host material DPEPO.

The blue-emitting Ir(III) metal complexes 1–5 were successfully obtained by simply heating both prochelat precursors, with  $\text{IrCl}_3 \cdot 3\text{H}_2\text{O}$  and KOAc in refluxing propionic acid (see the Supporting Information for details). This one-pot synthetic protocol offers much better product yields compared to the original procedures.<sup>[14]</sup> In the X-ray structure of  $[\text{Ir}(\text{mbib})(\text{pzpyOph}^{\text{F}})]$  4 (Figure S1, Supporting Information), the enlarged terminal-to-terminal bite angle of  $\text{C-Ir-N} = 168.25(14)^\circ$  involving the  $\text{pzpyOph}^{\text{F}}$  chelate suggests a reduced geometrical distortion compared to other Ir(III) complexes with 6-pyrazolyl-2-phenylpyridine chelates ( $\approx 157^\circ$ ) and this distortion is believed to be beneficial to the increased ligand field strength and reduced quenching of the emission.<sup>[20]</sup>

The absorption spectra of all five Ir(III) complexes in  $\text{CH}_2\text{Cl}_2$  solutions are depicted in Figure 1, while Table 1 lists the respective photophysical data. Complexes 3–4 exhibit more intense absorption peaks in the shorter wavelength region (260–350 nm) than other analogues due to the benzo substituents present in the pincer dicarbene chelate. The weaker absorption peaks occurring in the 350–430 nm region are attributed to the mixed singlet and triplet metal-to-ligand charge transfer (MLCT) transitions in all five complexes.

The five bis-tridentate Ir(III) metal complexes 1–5 show emission onsets at  $\approx 425 \text{ nm}$ , peak maxima at  $\approx 472 \text{ nm}$ , and two weak shoulders at  $\approx 448$  and  $505 \text{ nm}$  and emission full width at half maxima (FWHM) of  $\approx 3330$ – $3700 \text{ cm}^{-1}$  (Figure 2 and Table 1). The very shifting of emission maxima implies that the substituents in these complexes have little effect on the emission color. The emission of 2 differs slightly from other Ir(III) complexes with a less structured profile and the peak maximum is redshifted to  $478 \text{ nm}$ . All emission spectra of these complexes are clearly blue shifted versus the emission spectrum for the Ir(III) reference SB as shown in Figure 2.

The high emission quantum yields ( $\Phi$ ) of all studied complexes 1–5 are fostered by the rigidified skeleton of the bis-tridentate architecture.<sup>[11]</sup> Their phosphorescent nature ( $S_0 \leftarrow T_1$ ) is verified by the drastic oxygen quenching in aerated solution and long emission lifetime recorded upon degassing (Table 1). The observed emission lifetimes of 3 and 4 are found to be substantially longer than their counterparts 1 and 2 apparently due to the enhanced conjugation of the benzimidazolyldiene (vs imidazolyldiene) fragments. This fused ring conjugation

leads to a lowered electron density at the Ir(III) metal center and, hence, reduced MLCT character at the excited state. The reduced emission lifetimes for 2 and 5 ( $\tau_{\text{obs}} = 4.4$  and  $8.7 \mu\text{s}$ ) in  $\text{CH}_2\text{Cl}_2$  at RT indicate greater MLCT contributions in these complexes compared to 1, 3, and 4 ( $\tau_{\text{obs}}$  from 19 to  $61 \mu\text{s}$ ). Therefore, Ir(III) complexes 2 and 5 are considered to be the most suitable OLED emitters (for comparison, SB has an observed lifetime of  $5.4 \mu\text{s}$ ).

Cyclic voltammetry studies on 1–5 reveal reversible oxidation and irreversible reduction waves (Figure S2, Supporting Information) with data summarized in Table 1. Complexes 1 and 3 have more positive redox potentials compared to 2, 4, and 5, in accord with the attachment of electron-withdrawing ( $\text{CF}_3$ ) and electron-donating ( $\text{Bu}^t$ ) groups. Comparison between 2 and 5, where the complexes differ only by the presence of an additional  $\text{Bu}^t$  group at the pyridyl group of the phenoxy-containing tridentate chelate in 5, shows similar oxidation potentials but different reduction potentials by  $0.16 \text{ V}$ .

Electronic structure calculations on the five Ir(III) complexes 1–5 indicate the LUMO to be at both the pyrazolyl and pyridyl unit of 6-pyrazolyl-2-phenoxyphenylpyridine chelate in all cases (Figure 3 and Figure S3 and Table S2 and S3 (Supporting Information)). This is in contrast with the LUMO of SB which is

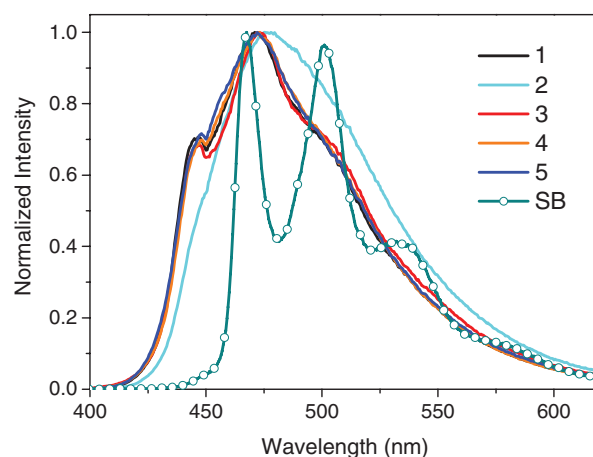


**Figure 2.** Normalized emission spectra of Ir(III) complexes 1–5 and SB recorded in degassed  $\text{CH}_2\text{Cl}_2$  at RT.

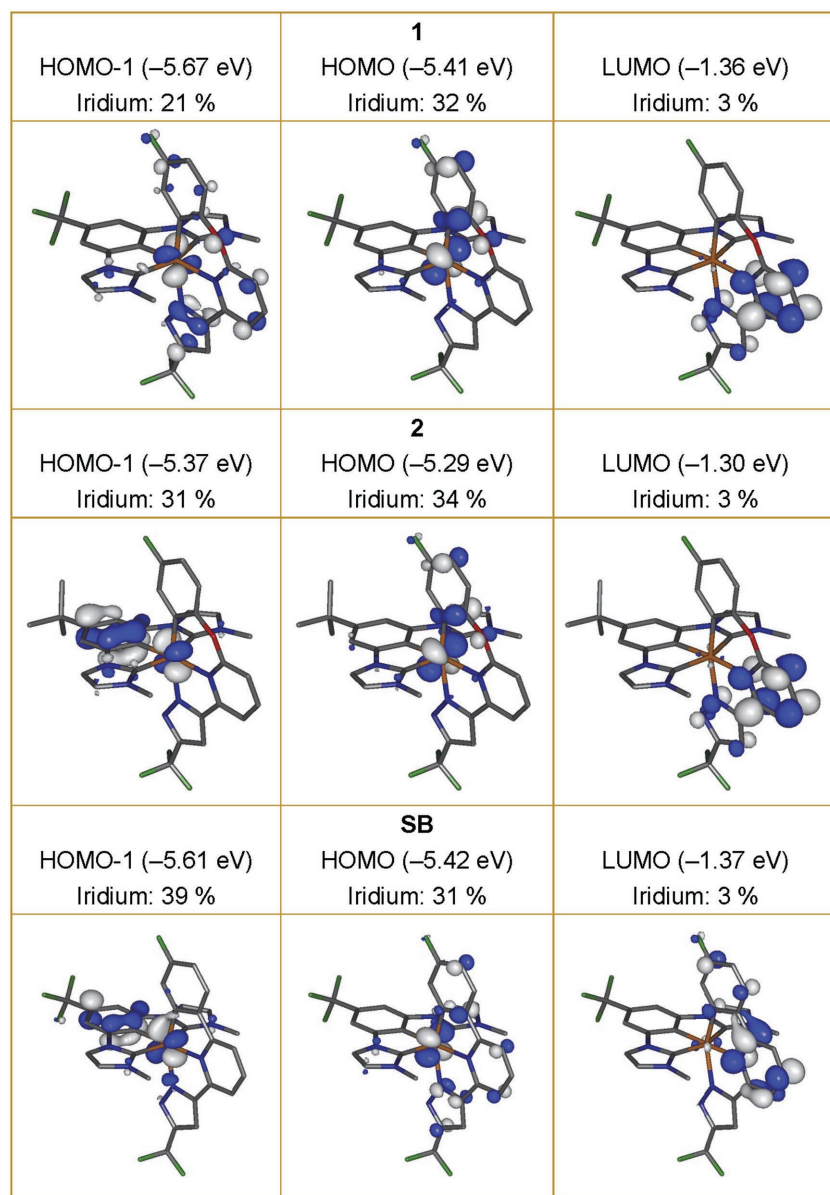


**Figure 3.** Plots of the frontier orbitals for Ir(III) complexes **1**, **2**, and **SB** with MO energies and % iridium MO contributions. All contours are plotted at  $\pm 0.06$  ( $e \text{ bohr}^{-3}$ ) $^{1/2}$ . All hydrogen atoms are omitted for clarity.

located on the same pyridyl unit and with contribution from the fluorophenyl unit as shown in Figure 3.

The HOMOs of **1–5** are of mixed metal–ligand character with both the metal  $d\pi$  orbital and fluorophenoxy ring as the dominant contributor in all except **4** where the HOMO is on the phenyl group of the dicarbene pincer moiety. In turn, the HOMO–1 in **4** has mixed metal–ligand character with electron contribution similar to the HOMO of all other complexes and is only 0.03 eV lower than HOMO in energy. The HOMO and HOMO–1 are also close in energy for the *tert*-butyl derivatives **2** and **5**.

The HOMO in **SB** differs from the HOMOs in **1–5** where the HOMO in **SB** has contributions from all units of the pzpyph<sup>F</sup> chelate (Figure 3). The computed HOMO and LUMO energies for **SB** are identical to those for **1**. This is remarkable

as different observed lowest energy absorption bands and emission maxima for these complexes usually reflect different HLGs. Our objective of widening the HLG energy using a nonconjugated chelate was therefore not supported by electronic structure calculations. These computations suggest that absorption and emission energies are not correctly predicted from calculated HLG energies but, as discussed later, are correctly predicted by time-dependent hybrid density functional theory (TD-DFT) calculations.

The agreement between computed HOMO energies of **1–5** and observed oxidation potentials of **1–5** from cyclic voltammetry is excellent (Table S2, Supporting Information). The trend between the LUMO energies of **1–5** fits well to the reduction wave potentials of **1–5**. The observed difference of 0.16 V in the reduction potentials between **2** and **5** is mirrored by the difference of 0.16 V in the LUMO energies of **2** and **5** supporting the fact that the LUMO is mainly on the central pyridyl ring of the dianionic chelate. The electron-withdrawing CF<sub>3</sub> group of dicarbene pincer chelate clearly lowers the frontier orbital energies while the electron-donating *tert*-butyl group raises the frontier orbital energies.

The relationship between the metal contribution in the MLCT excited state and emission lifetime is confirmed by molecular orbital (MO) computations here. The metal contributions in both HOMO and HOMO–1 are highest for **2** and lowest for **3** (Table S2 and Figure S2 and S3, Supporting Information) where **2** and **3** have the shortest and longest observed emission lifetimes, respectively (Table 1). TD-DFT computations on all complexes **1–5** and **SB** gave predicted wavelengths in excellent agreement with the observed deep-blue emissions from the class of nonconjugated complexes **1–5** and the sky-blue emitting **SB** (Table 2). The differences in the emission colors between these complexes are attributed to the different frontier orbital makeups **1–5** and reference **SB** where the oxygen atom breaks up the conjugation of chromophoric chelate in the former complexes.

These characteristics indicate their high potential in fabrication of true-blue emitting OLEDs. Initially we employed 9-(3-(9*H*-carbazol-9-yl)phenyl)-9*H*-carbazole-3-carbonitrile (mCPCN)<sup>[14,21,22]</sup> as host that has a relatively large triplet gap ( $E_T$ ) of 2.9 eV, and with characteristics similar to those of the wide triplet gap hosts *N,N*-dicarbazolyl-3,5-benzene (mCP) and 4,4'-bis(3-methylcarbazol-9-yl)-2,2'-biphenyl (mCBP) (Figure S4, Supporting Information).<sup>[5,22]</sup> When Ir(III) emitters were doped in mCPCN host (12 wt%), only complex **2** exhibited a PLQY value comparable to that recorded in solution, while all other



**Table 2.** Calculated metal MO contributions and  $S_0 \rightarrow S_1$ ,  $S_0 \rightarrow T_1$ , and  $S_0 \leftarrow T_1$  transition wavelengths (in nm) for 1–5 and SB with observed absorption (abs) and emission (em) maxima included for comparison.

	$\text{Ir}^{3+}$ [%]	$S_0 \rightarrow S_1$ [nm]	Oscillator strength ( $f$ )	Observed $\lambda_{\text{max}}$ (abs) <sup>b)</sup> [nm]	$S_0 \rightarrow T_1$ [nm]	Observed $\lambda_{\text{max}}$ (abs) <sup>c)</sup> [nm]	$S_0 \leftarrow T_1$ [nm]	Observed $\lambda_{\text{max}}$ (em) <sup>d)</sup> [nm]
1	27	368	0.0132	384	418	418	445	447
2	33	375	0.0096	388	417	420	444	448
3	26	362	0.0277	387	424	404	451	447
4	27	366	0.0020	387	423	419	450	448
		368 ( $S_0 \rightarrow S_2$ )	0.0185					
5	32	365	0.0136	386	412	412	438	448
SB	35	380	0.0243	401	442	431	470	467

<sup>a)</sup>From HOMO–1 and HOMO; <sup>b)</sup>MLCT band; <sup>c)</sup>MLCT band; <sup>d)</sup>Highest energy emission maximum.

complexes (1, 3–5) with more blue emissions gave relatively reduced PLQYs. This is probably associated with a poor host-to-guest energy transfer due to an inefficient host/guest spectral overlap and poor triplet exciton confinement due to the reduced host/guest triplet energy gap (Figure S5, Supporting Information). We then turned to bis[2-(diphenylphosphino)phenyl] ether oxide (DPEPO) as host with an even larger triplet gap of  $E_T$  of 3.35 eV,<sup>[21]</sup> in which PLQYs of 81% and 91% and emission lifetimes of 3.83 and 3.98  $\mu\text{s}$  were observed for 2 and 5, respectively (Table 1 and Figure S6 (Supporting Information)). Thus the OLEDs were best fabricated using the architecture: ITO/MoO<sub>3</sub> (1 nm)/TAPC (40 nm)/mCP (10 nm)/DPEPO doped with 2 or 5 (12 wt%, 20 nm)/3TPYMB (50 nm)/LiF (1 nm)/Al (100 nm), for which TAPC, mCP and 3TPYMB stand for 1,1-bis[(di-4-tolylamino)phenyl]cyclohexane, *N,N*-dicarbazolyl-3,5-benzene and tris-[3-(3-pyridyl)mesityl]borane, respectively, and served either as the hole- or electron-transport layers (Figure 4).<sup>[22]</sup> Vacuum-deposited DPEPO thin film doped with 2 or 5 constituted the emitting layer. The HOMO/LUMO levels of –5.33 eV/–2.39 eV for 2 and –5.32 eV/–2.31 eV for 5, obtained from the electrochemical data and the onset of the absorption/emission spectra, are both within the corresponding energy levels of the DPEPO host.

Figure 5a–d shows representative electroluminescence (EL) characteristics of OLEDs for 2 and 5, while performance parameters of both devices are summarized in Table S4 (Supporting Information). The EL spectra are similar to their PL spectra, indicating pure EL from either 2 or 5 and presenting CIE<sub>(x,y)</sub> coordinates of (0.15, 0.24) and (0.15, 0.17) for 2 and 5, respectively. The further blueshifted EL from 5 relative to 2 is again consistent with their PL characteristics. These devices in general exhibit a relatively low turn-on voltage of  $\approx 2.5$ –3 V and an operation voltage of 5–5.2 V for a practical brightness of 100 cd m<sup>–2</sup>. The devices containing 2 and 5 show EL efficiencies of up to (19.7%, 33.5 cd A<sup>–1</sup>, 26.3 lm W<sup>–1</sup>) and (20.7%, 28.8 cd A<sup>–1</sup>, 22.6 lm W<sup>–1</sup>), respectively. The superior EQE of 5 (vs 2) is consistent with the higher PLQY of 5 in thin films, while lower current and power efficiencies of 5 are mainly associated with its deeper blue emission (vs 2). With an EQE of >20% and a CIE<sub>(x,y)</sub> of (0.15, 0.17) from 5, to our knowledge, these results represent the best deep-blue EL from the bis-tridentate Ir(III) complexes, and they are also comparable to the best blue OLEDs

using bis-tridentate Ir(III) complexes recorded at practical brightness of 100 cd m<sup>–2</sup>. Notably, the EL from 2 and 5 are significantly blueshifted versus the EL from SB with an identical architecture as shown in Figure 5a,b.

In summary, the deep-blue-emitting, bis-tridentate Ir(III) phosphors with emission peak maxima in the region of 470 nm were assembled using both dicarbenic pincer ancillary and chromophoric 6-pyrazolyl-2-phenoxy-pyridine chelate with a partially interrupted  $\pi$ -conjugation. Hybrid-DFT and TD-DFT computations reveal that this interrupted conjugation changes the nature of the frontier orbitals with respect to the sky-blue-emitting SB with 6-pyrazolyl-2-phenylpyridine chelate. Furthermore, a good correlation was obtained between the emission lifetime and carbene ancillaries: those with imidazolylidene and *tert*-butyl substituents (i.e., 2 and 5) exhibited reduced lifetimes against those with either benzimidazolylidene or CF<sub>3</sub> substituents (i.e., 1, 3, and 4), due to the varied MLCT contributions at the lowest energy excited states. Overall, OLEDs with dopants 2 and 5 gave excellent performances in all aspects, and shed light on how to develop similar deep-blue-emitting OLED phosphors for future industrial applications.

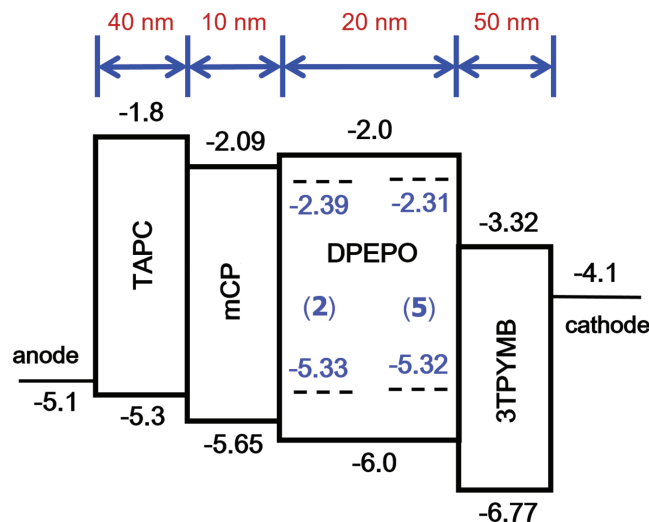


**Figure 4.** Device configuration and relative energy levels of materials used in OLEDs.

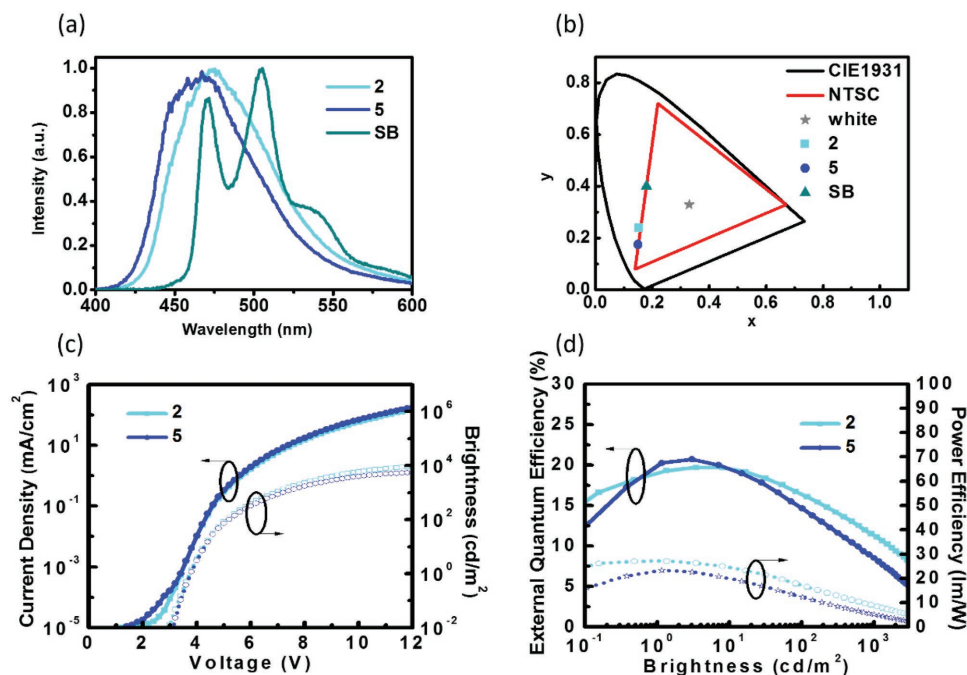


**Figure 5.** a,b) EL spectra and 1931 CIE<sub>(x,y)</sub> coordinates, for which the respective data for SB are also included; c) current–voltage–luminance (*I*–*V*–*L*) characteristics and d) external quantum efficiencies (EQEs) and power efficiencies of devices 2 and 5 at the doping conc. of 12 wt%.

## Supporting Information

Supporting Information is available from the Wiley Online Library or from the author.

## Acknowledgements

H.-H.K., Y.-T.C., and L.R.D. contributed equally to this work. Y.C. acknowledges the Ministry of Science and Technology, Taiwan for funding, 106-2811-M-007-023.

## Conflict of Interest

The authors declare no conflict of interest.

## Keywords

carbene, iridium, organic light-emitting diodes, phosphorescence, pyrazole, tridentate

Received: May 3, 2017  
Revised: May 22, 2017  
Published online: June 21, 2017

- [1] a) L. Xiao, Z. Chen, B. Qu, J. Luo, S. Kong, Q. Gong, J. Kido, *Adv. Mater.* **2011**, 23, 926; b) K. Li, G. S. Ming Tong, Q. Wan, G. Cheng, W.-Y. Tong, W.-H. Ang, W.-L. Kwong, C.-M. Che, *Chem. Sci.* **2016**, 7, 1653; c) C.-W. Lu, Y. Wang, Y. Chi, *Chem. – Eur. J.* **2016**, 22, 17892.  
[2] a) W.-C. Chen, C.-S. Lee, Q.-X. Tong, *J. Mater. Chem. C* **2015**, 3, 10957; b) T. Fleetham, G. Li, J. Li, *Adv. Mater.* **2017**, 29, 1601861.

- [3] Y. Im, S. Y. Byun, J. H. Kim, D. R. Lee, C. S. Oh, K. S. Yook, J. Y. Lee, *Adv. Funct. Mater.* **2017**, 27, 1603007.  
[4] E. D. Baranoff, B. Curchod, *Dalton Trans.* **2015**, 44, 8318.  
[5] a) X. Yang, X. Xu, G. Zhou, *J. Mater. Chem. C* **2015**, 3, 913; b) Y. Zhang, J. Lee, S. R. Forrest, *Nat. Commun.* **2014**, 5, 5008; c) J. Lee, H.-F. Chen, T. Batagoda, C. Coburn, P. I. Djurovich, M. E. Thompson, S. R. Forrest, *Nat. Mater.* **2016**, 15, 92.  
[6] S. Scholz, D. Kondakov, B. Lüssem, K. Leo, *Chem. Rev.* **2015**, 115, 8449.  
[7] V. L. Whittle, J. A. G. Williams, *Dalton Trans.* **2009**, 3929.  
[8] T. Yutaka, S. Obara, S. Ogawa, K. Nozaki, N. Ikeda, T. Ohno, Y. Ishii, K. Sakai, M. Haga, *Inorg. Chem.* **2005**, 44, 4737.  
[9] N. Darmawan, C.-H. Yang, M. Mauro, M. Raynal, S. Heun, J. Pan, H. Buchholz, P. Braunstein, L. De Cola, *Inorg. Chem.* **2013**, 52, 10756.  
[10] R. G. Alabau, B. Eguillor, J. Esler, M. A. Esteruelas, M. Oliván, E. Oñate, J.-Y. Tsai, C. Xia, *Organometallics* **2014**, 33, 5582.  
[11] J. A. Treadway, B. Loeb, R. Lopez, P. A. Anderson, F. R. Keene, T. J. Meyer, *Inorg. Chem.* **1996**, 35, 2242.  
[12] Y. Chi, T.-K. Chang, P. Ganesan, P. Rajakannu, *Coord. Chem. Rev.* **2017**, 346, 91.  
[13] a) B. Tong, H. Y. Ku, I. J. Chen, Y. Chi, H.-C. Kao, C.-C. Yeh, C.-H. Chang, S.-H. Liu, G.-H. Lee, P.-T. Chou, *J. Mater. Chem. C* **2015**, 3, 3460; b) J. Lin, N.-Y. Chau, J.-L. Liao, W.-Y. Wong, C.-Y. Lu, Z.-T. Sie, C.-H. Chang, M. A. Fox, P. J. Low, G.-H. Lee, Y. Chi, *Organometallics* **2016**, 35, 1813.  
[14] C.-Y. Kuei, W.-L. Tsai, B. Tong, M. Jiao, W.-K. Lee, Y. Chi, C.-C. Wu, S.-H. Liu, G.-H. Lee, P.-T. Chou, *Adv. Mater.* **2016**, 28, 2795.  
[15] C.-Y. Kuei, S.-H. Liu, P.-T. Chou, G.-H. Lee, Y. Chi, *Dalton Trans.* **2016**, 45, 15364.  
[16] Y.-H. Song, Y.-C. Chiu, Y. Chi, Y.-M. Cheng, C.-H. Lai, P.-T. Chou, K.-T. Wong, M.-H. Tsai, C.-C. Wu, *Chem. – Eur. J.* **2008**, 14, 5423.  
[17] a) C.-F. Chang, Y.-M. Cheng, Y. Chi, Y.-C. Chiu, C.-C. Lin, G.-H. Lee, P.-T. Chou, C.-C. Chen, C.-H. Chang, C.-C. Wu, *Angew. Chem., Int. Ed.* **2008**, 47, 4542; b) Y.-C. Chiu, J.-Y. Hung,

- Y. Chi, C.-C. Chen, C.-H. Chang, C.-C. Wu, Y.-M. Cheng, Y.-C. Yu, G.-H. Lee, P.-T. Chou, *Adv. Mater.* **2009**, *21*, 2221; c) Y.-C. Chiu, Y. Chi, J.-Y. Hung, Y.-M. Cheng, Y.-C. Yu, M.-W. Chung, G.-H. Lee, P.-T. Chou, C.-C. Chen, C.-C. Wu, H.-Y. Hsieh, *ACS Appl. Mater. Interfaces* **2009**, *1*, 433; d) L. He, L. Duan, J. Qiao, G. Dong, L. Wang, Y. Qiu, *Chem. Mater.* **2010**, *22*, 3535; e) C.-H. Yang, M. Mauro, F. Polo, S. Watanabe, I. Muenster, R. Fröhlich, L. De Cola, *Chem. Mater.* **2012**, *24*, 3684; f) Y. Kang, Y.-L. Chang, J.-S. Lu, S.-B. Ko, Y. Rao, M. Varlan, Z.-H. Lu, S. Wang, *J. Mater. Chem. C* **2013**, *1*, 441; g) F. Kessler, Y. Watanabe, H. Sasabe, H. Katagiri, M. K. Nazeeruddin, M. Grätzel, J. Kido, *J. Mater. Chem. C* **2013**, *1*, 1070; h) S. Lee, S.-O. Kim, H. Shin, H.-J. Yun, K. Yang, S.-K. Kwon, J.-J. Kim, Y.-H. Kim, *J. Am. Chem. Soc.* **2013**, *135*, 14321; i) J. Frey, B. F. E. Curchod, R. Scopelliti, I. Tavernelli, U. Rothlisberger, M. K. Nazeeruddin, E. Baranoff, *Dalton Trans.* **2014**, *43*, 5667; j) K. S. Bejoymohandas, A. Kumar, S. Varughese, E. Varathan, V. Subramanian, M. L. P. Reddy, *J. Mater. Chem. C* **2015**, *3*, 7405; k) T. Duan, T.-G. Chang, Y. Chi, J.-Y. Wang, Z.-N. Chen, W.-Y. Hung, C. H. Chen, G.-H. Lee, *Dalton Trans.* **2015**, *44*, 14613; l) J.-H. Lee, G. Sarada, C.-K. Moon, W. Cho, K.-H. Kim, Y. G. Park, J. Y. Lee, S.-H. Jin, J.-J. Kim, *Adv. Opt. Mater.* **2015**, *3*, 211; m) T.-Y. Li, X. Liang, L. Zhou, C. Wu, S. Zhang, X. Liu, G.-Z. Lu, L.-S. Xue, Y.-X. Zheng, J.-L. Zuo, *Inorg. Chem.* **2015**, *54*, 161; n) Y.-H. Kim, J.-B. Kim, S.-H. Han, K. Yang, S.-K. Kwon, J.-J. Kim, *Chem. Commun.* **2015**, *51*, 58; o) Y. Nagai, H. Sasabe, S. Ohisa, J. Kido, *J. Mater. Chem. C* **2016**, *4*, 9476; p) Y. Feng, X. Zhuang, D. Zhu, Y. Liu, Y. Wang, M. R. Bryce, *J. Mater. Chem. C* **2016**, *4*, 10246; q) Y.-J. Cho, S.-Y. Kim, J.-H. Kim, J. Lee, D. W. Cho, S. Yi, H.-J. Son, W.-S. Han, S. O. Kang, *J. Mater. Chem. C* **2017**, *5*, 1651.
- [18] V. C. Vargas, R. J. Rubio, T. K. Hollis, M. E. Salcido, *Org. Lett.* **2003**, *5*, 4847.
- [19] D. Maiti, S. L. Buchwald, *J. Org. Chem.* **2010**, *75*, 1791.
- [20] L. Hammarström, F. Barigelli, L. Flamigni, M. T. Indelli, N. Armaroli, G. Calogero, M. Guardigli, A. Sour, J.-P. Collin, J.-P. Sauvage, *J. Phys. Chem. A* **1997**, *101*, 9061.
- [21] a) Q. Zhang, B. Li, S. Huang, H. Nomura, H. Tanaka, C. Adachi, *Nat. Photonics* **2014**, *8*, 326; b) Y.-J. Hsu, Y.-T. Chen, W.-K. Lee, C.-C. Wu, T.-C. Lin, S.-H. Liu, P.-T. Chou, C.-W. Lu, I. C. Cheng, Y.-J. Lien, Y. Chi, *J. Mater. Chem. C* **2017**, *5*, 1452.
- [22] a) M.-S. Lin, S.-J. Yang, H.-W. Chang, Y.-H. Huang, Y.-T. Tsai, C.-C. Wu, S.-H. Chou, E. Mondal, K.-T. Wong, *J. Mater. Chem.* **2012**, *22*, 16114; b) W.-L. Tsai, M.-H. Huang, W.-K. Lee, Y.-J. Hsu, K.-C. Pan, Y.-H. Huang, H.-C. Ting, M. Sarma, Y.-Y. Ho, H.-C. Hu, C.-C. Chen, M.-T. Lee, K.-T. Wong, C.-C. Wu, *Chem. Commun.* **2015**, *51*, 13662.